[16]H. Daniel, W. Collin, M. Kuntze, S. Margulies, B. Martin, O. Mehling, P. Schmidln, and H. Schmitt, Nucl. Phys. A118, 689 (1968).

[17]R. Tickle and J. Bardwick, Phys. Rev. 178, 2006 (1969).

[18]L. S. Kisslinger and R. A. Sorensen, Rev. Mod. Phys. 35, 853 (1963).

[19]G. H. Fuller and V. W. Cohen, Nucl. Data A5, 433 (1969).

[20]R. Kalish, R. R. Borchers, and H. W. Kugel, Nucl. Phys. A161, 637 (1970).

[21]F. Smend, W. D. Schmidt-Ott, and A. Flammersfeld, Z. Physik 185, 426 (1965).

[22]B. Jung and J. Svedberg, Arkiv Fysik 19, 429 (1961).

[23]M. J. Martin, Nucl. Data B5(No. 6), 601 (1971).

[24]R. L. Auble, Nucl. Data B5(No. 6), 581 (1971).

[25]J. H. Bjerregaard, O. Hansen, and O. Nathan, Nucl. Phys. A94, 457 (1967).

Photoproton Reaction on Sn Isotopes

M. Sugawara, K. Shoda, T. Saito, H. Miyase, A. Suzuki, and S. Oikawa

Laboratory of Nuclear Science, Faculty of Science, Tohoku University, Sendai, Japan

and

R. Bergère

Centre d'Etudes Nucléaires de Saclay, Saclay, France

(Received 2 August 1971)

The photoproton spectra and the photoproton yield curves have been measured for ^{116}Sn, ^{117}Sn, ^{118}Sn, ^{120}Sn, ^{122}Sn, and ^{124}Sn using the electrodisintegration reaction. Several proton peaks through isobaric analog states are found in each proton spectrum. In ^{120}Sn it was found that 8.3- and 8.0-MeV proton groups were emitted from an analog state at 19.2 MeV. For the other isotopes the excitation energies of the analog states were also estimated by assuming the same decay mode as that of ^{120}Sn. The yield curves of protons with an energy from 5.1 to 10.2 MeV have two breaks at each isotope corresponding to isobaric analog states. The excitation energies and the integrated cross sections were also determined.

I. INTRODUCTION

In medium and heavy nuclei the (γ, p) reactions offer a useful means to study the $E1$ analog states, since these states decay preferentially through proton emission rather than neutron emission because of the isospin selection rule.[1] Analog states are expected to have a width of several tens of keV, so that the (γ, p) reaction cross sections might represent sharp resonant structures. When one measures proton spectra with an instrument having sufficient resolution, sharp proton peaks from analog states are found over the continuous proton background which comes from the ordinary $E1$ giant resonance. The yield of the proton background is very low in these nuclei, so it is easy to distinguish protons through analog states from others. In addition to the interesting phenomena of the $E1$ analog states from the point of view of the giant resonance, their spins and parities and their various decay widths offer valuable information as to the structure of the corresponding parent states as discussed everywhere.

Some experimental examples have already been reported by the present authors.[2] However, no systematic study of the $E1$ analog states on isotopes has been undertaken so far. Tin isotopes are suitable for such a study, because there are many isotopes which differ from each other by only one neutron. Moreover, their closed proton shell simplifies the interpretation of the dependence of analog states on neutron number.

Up to now, several (γ, p) experiments have been carried out on tin isotopes. Kuo and Ratner[3] measured the (γ, p) cross section on ^{120}Sn and also studied the excitation mode of the (γ, p) giant dipole resonance by measuring the yield ratio for the ground state to the isomeric state in ^{119}In. Yuta and Morinaga[4] and Hummel[5] studied the same ratios in the residual nuclei for ^{118}Sn, ^{120}Sn, ^{122}Sn, and ^{124}Sn. Osokina[6] measured proton spectra using nuclear emulsions and found gross proton peaks around 8 MeV.

II. EXPERIMENTAL PROCEDURES

The present measurements of photoprotons were made by using the electrodisintegration phenomena. Reaction targets were bombarded directly by electrons from the intermediate sta-

tion of the Tohoku 300-MeV linear accelerator.[7]
This type of experiment seems to be convenient
from an experimental point of view, although a
little theoretical ambiguity appears in the process
of extracting the (γ, p) cross section from that of
electrodisintegration as explained in several
articles.[8] The beam handling is easier than in
the case of bremsstrahlung, so that one can real-
ize a small beam size at the reaction target with-
out losing the current intensity, which is a nec-
essary condition for obtaining high-resolution
proton spectra with our apparatus.

A broad-range magnetic spectrometer of the
Browne-Buchner type was used.[7, 9] The radius
of the central orbit is 55 cm, which is equal to
the radius of the circular pole pieces with a gap
of 3 cm. In the focal plane, 100 solid-state de-
tectors are arranged to detect protons. Each de-
tector consists of a lithium-drifted silicon diode
with dimensions 10 mm long, 2 mm wide, and
1 mm thick. The energy bin defined by each de-
tector width is 0.36% and the energy interval from
one channel to the next is 0.72% at the central
orbit. Moreover the whole detector ladder can
be shifted along the focal plane in steps of 0.36%.
The detectors are followed by a buffer register
connected to a direct-access system of an on-line
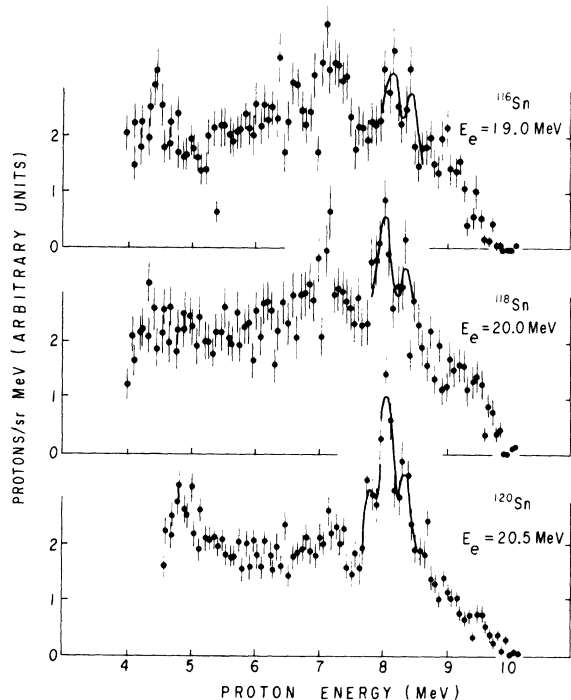computer through preamplifiers, main amplifiers,

and discriminators. The solid angle viewed by a
detector at the central orbit is about 7×10^{-4} sr,
which is defined by the opening of the slit system,
the pole gap, and the dimension of the detector.
These values were checked with the ^{2}H(γ, p) reac-
tion.

The beam current was monitored by a secondary-
emission chamber calibrated by a Faraday cup
which was removed from the beam line during
proton measurements to avoid an increase of the
background. The beam position and the beam
size were checked before each run by observing
the luminescence of a BeO plate which replaced
the target by means of a remote-control system.

Self-supporting metal foils of tin isotopes with
mass numbers 116, 117, 118, 120, 122, and 124
(enriched to 95.7, 78.8, 96.6, 98.4, 92.3, and
94.7% and rolled to 4.7-, 4.7-, 5.1-, 5.0-, 5.1-,
and 5.6-mg/cm^2 thickness, respectively) were
bombarded with an electron beam kept lower than
2 μA to avoid melting of the targets.

In the electrodisintegration process, the nu-
cleus is excited by virtue of the interaction with
the electron's electromagnetic field. Neglecting
the small contributions of large momentum trans-
fer, the (γ, p) cross sections can be extracted
from the corresponding electrodisintegration
cross section by Eq. (1), according to the virtual-
photon theory[8, 10-13]:

$$\sigma_{(e,e'p)}(E_e) = \int_0^{E_e} \sigma_{(\gamma,p)}(E) N(E, E_e) dE , \qquad (1)$$

where $\sigma_{(e,e')}(E_e)$ is the cross section of electrodis-
integration for an electron energy E_e; $\sigma_{(\gamma,p)}(E)$ is
the (γ, p) cross section at a photon energy E; and
$N(E, E_e)$ is the number of the virtual photons with
an energy E corresponding to an electron of the en-
ergy E_e. The virtual-photon spectra were calcu-
lated using a formula introduced by Barber under
the assumption of a point charge.[11] $N(E, E_e)$ has a
spectrum similar to that of bremsstrahlung and
depends on the multipolarity of the interaction.
If the cross section shows such a sharp resonance
$\sigma_{(\gamma,p)}^R$ that the virtual-photon spectrum can be ap-
proximated as constant in the vicinity of the reso-
nance, the proton yield through the resonance can
be given by

$$\Delta Y_{(e,e'p)}(E_e) = C N(E_x, E_e) \int \sigma_{(\gamma,p)}^R dE , \qquad (2)$$

where E_x is the energy of the resonance, and C
is a geometrical factor of the experiment.

FIG. 1. The proton spectra from ^{116}Sn, ^{118}Sn, and
^{120}Sn emitted over a solid angle of 4π. The spectra
were synthesized from the spectra measured at 38, 64,
90, 116, and 142°.

III. PROTON ENERGY SPECTRA

Proton energy spectra were measured at 38,
64, 90, 116, and 142° with respect to the incident

electron beam for ^{116}Sn, ^{118}Sn, and ^{120}Sn. The angular distributions of the protons integrated over the whole spectrum show slightly the asymmetry peaked at forward angles according to an interference between different multipolarities. However, it becomes possible to devise a procedure for integrating the emitted protons over a solid angle of 4π, since the general features of these spectra do not change abruptly between the successive angles mentioned above. Figure 1 represents such integrated proton spectra for ^{116}Sn, ^{118}Sn, and ^{120}Sn. Figure 2 shows differential proton spectra for ^{117}Sn and ^{124}Sn measured at 90° and for ^{122}Sn measured at 125.3°.

A characteristic of these spectra is that each isotope has prominent proton peaks around 8 MeV except for ^{117}Sn. At least two peaks are found on ^{116}Sn, ^{118}Sn, ^{122}Sn, and ^{124}Sn; and three peaks on ^{120}Sn as indicated by the solid lines in the figures. The energies of the proton peaks are listed in column 2 of Table I. An additional set of experimental points for the ^{120}Sn measurements was obtained by shifting the detector ladder by 0.36% in energy in order to make the shapes of the peaks clear. Figure 3 gives the results obtained at 125.3° for incident electron energies of 20.5, 19.5, and 19.1 MeV. The energies of the three proton peaks are found to be 8.3, 8.0, and 7.8 MeV. The peak widths at half maximum are about 200 keV.
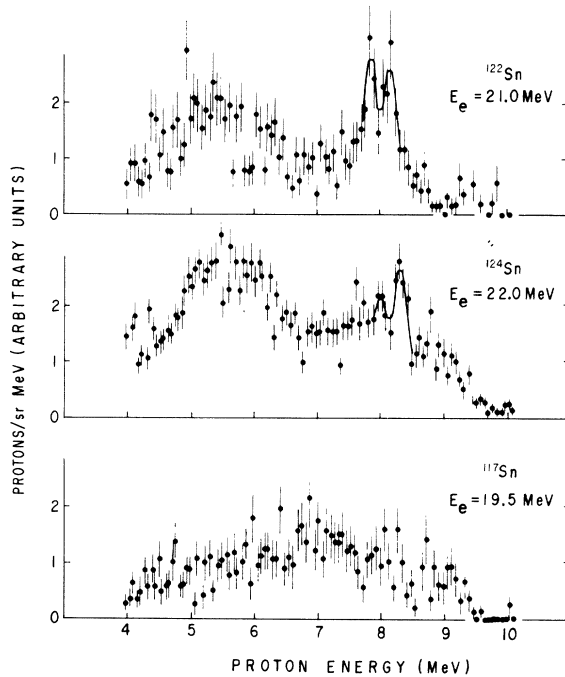
This fact suggests that the resonances from which these protons are emitted should have widths narrower than 100 keV because the corrections are 80 keV for the resolution of the spectrometer and 150 keV for the energy loss of protons in the reaction target. According to the dependence of the number of protons in these peaks on the incident electron energy, the 8.3- and 8.0-MeV protons come from one resonant state at an excitation energy of 19.2 ± 0.2 MeV and leave the residual ^{119}In nucleus in the ground state and in the first excited state at 300 keV, respectively.[14] The protons at 7.8 MeV could not be assigned to the same state mentioned above, because of the small counting rate, but they are tentatively considered to be emitted from the same state leaving the residual nucleus in a higher excited state.

The decay scheme is presented in Fig. 4 with several related nuclear states. The resonant state at 19.2 MeV was assigned to an analog state having isospin $T + 1$ (T is the isospin of the ground state) and assumed to have spin and parity 1$^-$, because such a narrow level width in the highly excited energy region can be attributed only to the isobaric analog state, and a strong transition takes place in most cases through an $E1$ process in the photoreactions. The angular distribution of protons in the peaks is symmetrical about 90° and decreases uniformly in the forward and backward directions. This does not contradict the $E1$ assumption, but is not enough to determine the multipolarity because of the large statistical fluctuation.

The integrated cross section $\int \sigma^R_{(\gamma, p)} dE$ summed over these three proton groups were obtained by using Eq. (2) and $E1$ virtual-photon spectrum.

FIG. 2. The proton spectra from ^{117}Sn, ^{122}Sn, and ^{124}Sn measured at 90, 125.3, and 90°, respectively.

TABLE I. Excitation energies and the integrated cross sections of the resonances from the proton spectra. The underlined numerals show the E_p of the most prominent proton peaks. The data were obtained from the yield of protons of $7.5 < E_p < 8.5$ MeV.

A	E_p (MeV)	E_x (MeV)	$\int \sigma^R dE$ (mb MeV)	$B(E1\uparrow)\Gamma_p/\Gamma$ (e^2 F^2)	E_x (In) (MeV)
116	$\underline{8.1}$ 8.4	17.7	0.6	0.008	1.8
118	8.0 $\underline{8.3}$	18.4	0.8	0.011	1.4
120	7.8 $\underline{8.0}$ 8.3	19.2	1.1	0.014	1.1
122	$\underline{7.9}$ 8.2	19.9	1.3	0.015	0.9
124	7.9 $\underline{8.2}$	21.0	0.9	0.010	1.0

The continuous part of the proton spectrum was subtracted by assuming this quantity as a mean value of those on both sides of the resonance. The correction due to the interference[15, 16] between the analog state and the ordinary giant resonance was neglected. For the other isotopes, the same decay schemes as for ^{120}Sn were assumed; the most prominent peaks, marked with underlines in Table I, leave the residual nucleus in the first excited state at 0.3 MeV, and all the proton peaks listed come from one analog state. The excitation energies E_x were estimated from the relation

$$E_x = \frac{A}{A-1} E_p + B_p + 0.3 \text{ MeV} , \qquad (3)$$

where E_p is the proton energy of the prominent peak and B_p is the proton separation energy. The
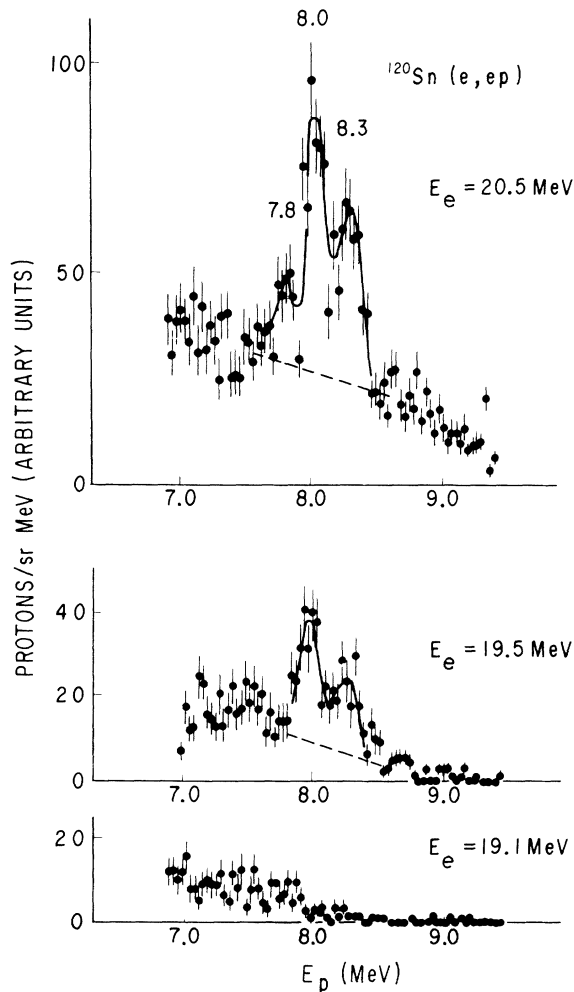
resulting excitation energies and the integrated cross sections are listed in the third and fourth column of Table I. The excitation energies are shown in Fig. 6 with open circles connected by dashed lines. The reduced transition probabilities $B(E1\uparrow)$ multiplied by the branching ratio of the observed proton channel to the total decay Γ_p/Γ were calculated from the integrated cross sections under the $E1$ assumption by

$$\int \sigma_{(\gamma,p)}^R dE = \frac{16}{9} \pi^3 \frac{E_x}{\hbar c} B(E1\uparrow) \frac{\Gamma_p}{\Gamma} . \qquad (4)$$

The branching ratio cannot be estimated since the proton decay to highly excited residual states, and other decay possibilities such as neutron emission, are not known for Sn isotopes. If $\Gamma_p/\Gamma = 1$, the lowest value of the reduced transition probability $B(E1\uparrow)$ can be evaluated by Eq. (4), since the branching ratio does not exceed 1. These reduced transition probabilities are represented

FIG. 3. The proton spectra from ^{120}Sn measured at 125.3° to obtain the isochromats of the proton peaks at 7.8, 8.0, and 8.3 MeV. The protons under the dashed lines are subtracted as background.
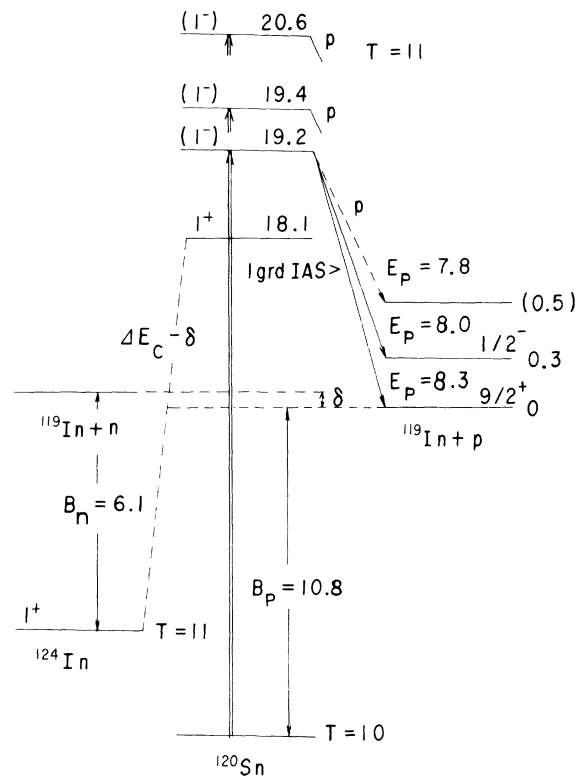

FIG. 4. The isobaric analog states obtained in the present experiment. The energies are indicated in units of MeV. The 19.2-MeV state was found in the study of proton spectra and decays to the residual states in ^{119}In by proton emission as shown. The states at 19.4 and 20.6 MeV were obtained from the yield curve of protons shown in Fig. 5. The excitation energy of the ground analog state | grd IAS⟩ was evaluated by using B_p, B_n, and ΔE_C. The mass difference between neutron and proton is denoted by δ.

with open circles in Fig. 7. In the same figure, the Weisskopf single-particle values of B_W are also shown for comparison. They are given by

$$B_W = \frac{9}{16\pi} \left(\frac{hc}{E_\gamma}\right)^3 \frac{\Gamma_W(E1)}{2T+2} .$$

According to Wilkinson's estimate,[17]

$$\Gamma_W(E1) = 6.8 \times 10^{-2} A^{2/3} E_\gamma^3 \text{ eV} .$$

From the two equations,

$$B_W = 0.065 \frac{A^{2/3}}{2T+2} e^2 \text{ F}^2 , \tag{5}$$

where T is the isospin of the ground state. The B_W are multiplied by a hindrance factor of $1/(2T+2)$.[16, 18]

IV. PROTON-YIELD CURVES

In order to obtain the yield curves, proton spectra were measured at an angle of 125.3° by changing the incident electron energies in 200- or 100-keV steps. The proton numbers within the energy range from 5.1 to 10.2 MeV were summed up. The small contributions of the lower- and the higher-energy protons outside of this energy region were neglected considering that these small parts cannot change seriously the general characteristics of the yield curves within the present
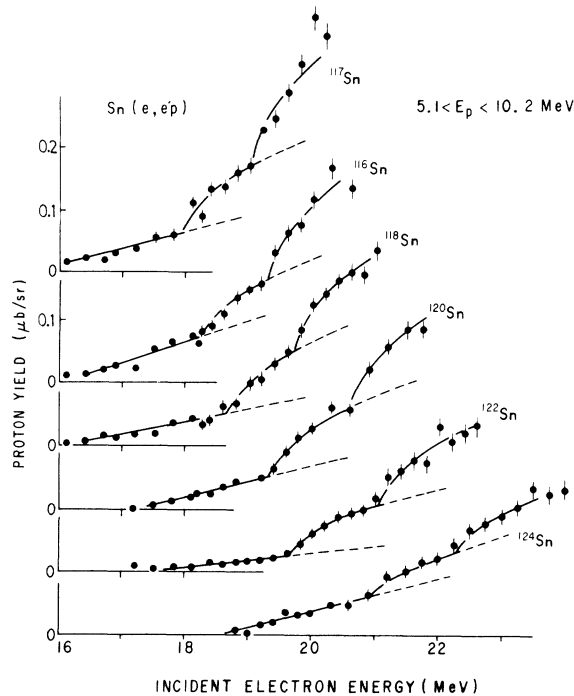
incident-energy range. The yield curves are shown in Fig. 5, where every curve has two breaks separated by about 1 MeV. These breaks are caused by the existence of resonant states with narrow level widths. The lower-energy ones lie near the (γ, np) reaction thresholds. But the possibility of relating these breaks to the threshold effect is rejected on the grounds that (γ, np) cross sections are negligibly small near the threshold because of the high Coulomb barrier for low-energy protons. This (γ, np) cross section was reported to reach a sizable value at an energy about 4 MeV higher than the threshold.[3]

If the cross section includes a sharp resonance $\sigma_{(\gamma,p)}^R$ at E_x standing out over the continuous cross section, the excess increase of the proton yield is proportional to the value given by Eq. (2). Thus the yield rises suddenly at $E_e = E_x$ and increases gradually with increasing electron energy E_e in proportion to the virtual-photon spectrum $N(E_x, E_e)$. In order to emphasize the contribution of the resonant state in the yield curves, the lower-energy sides of the yields were extrapolated linearly as shown by dashed lines in Fig. 5, and subtracted from the yields in the corresponding energy region. By substituting the remaining resonant state contribution $\Delta Y_{(e,e'p)}(E_e)$ into Eq. (2), one can obtain the integrated cross section $\int \sigma_{(\gamma,p)}^R dE$. The upper limit of the resonant level widths were also estimated at less than 300 keV by analyzing the rising shapes of the yield curves at the breaks, since the rising shapes are blunted by the energy spread of the incident electron beam and the level widths of the resonant states in question.

The total proton yields for the whole solid angle

FIG. 5. The yield curves of protons within 5.1 to 10.2 MeV measured at 125.3°. Two breaks in each curve correspond to the isobaric analog state.

TABLE II. Excitation energies and integrated cross sections of the resonant states estimated from the proton-yield curve.

A	E_x (MeV)	$\int \sigma^R dE$ (mb MeV)	$B(E1\uparrow)\Gamma_p/\Gamma$ (e^2 F^2)	E_x (In) (MeV)
116	18.3	3.0	0.040	2.4
	19.3	6.4	0.083	3.4
117	18.0	4.4	0.060	3.9
	19.0	7.4	0.097	4.9
118	18.7	4.9	0.065	1.7
	19.8	5.8	0.072	2.8
120	19.4	4.6	0.058	1.3
	20.6	5.7	0.068	2.5
122	19.7	3.8	0.048	0.7
	21.1	4.0	0.058	2.1
124	20.9	2.0	0.025	0.9
	22.3	2.9	0.032	2.3

were obtained by assuming that the angular distributions could be represented by $I(\theta) = a + bP_2(\cos\theta)$, which is fulfilled in the case of pure $E1$ excitation. Although the angular distributions of the total protons have an asymmetry peaked slightly at forward angles, the $P_1(\cos\theta)$ term was neglected in the present calculation on the grounds that the asymmetry may contribute mainly to the continuous parts of the cross section which can interfere with other excitation modes such as the electric quadrupole. However, this is not the case for the resonances. At the present angle of 125.3° the P_2 term, which does not contribute to the total yield, is automatically rejected, since $P_2(125.3°) = 0$. Then total cross sections can be given simply by multiplying the differential ones by 4π. The uncertainty of the excitation energies is estimated as 150 keV. This is attributed to the rather wide steps (100 or 200 keV) and to the spread of the incident electron energy (about 150 keV). The errors in the integrated cross sections are estimated at ±30% for the absolute values and are much better for relative values. In Table II the resulting integrated cross sections are given with

excitation energies. Reduced transition probabilities were also calculated on the assumption of $E1$ transition, and are given in column 4 of Table II. They are multiplied by the branching ratio Γ_p/Γ for reasons explained in the preceding section (Γ_p refers to protons between 5.1 to 10.2 MeV only). The excitation energies are shown in Fig. 6 by closed circles connected with solid lines. The reduced transition probabilities are presented by closed circles in Fig. 7.

V. DISCUSSION

Photoprotons from ^{114}Sn and ^{124}Sn were measured previously by Osokina[6] using nuclear emulsions. His proton spectra gave gross peaks around $E_p = 8$ MeV, but did not show any fine structures, because of the energy resolution of about 500 keV. In the present studies three sharp proton peaks were found for ^{120}Sn. Two of them are identified as protons coming from an analog state at 19.2 MeV and leaving the residual ^{119}In nucleus in the ground state $\frac{9}{2}^+$ and the first excited state $\frac{1}{2}^-$, which are well described as proton-hole states in the $1g_{9/2}$ and $2p_{1/2}$ shells. The branching ratio of protons leaving the $(1g_{9/2})^{-1}$ state to that leaving the $(2p_{1/2})^{-1}$ state is about 0.6, which is esti-
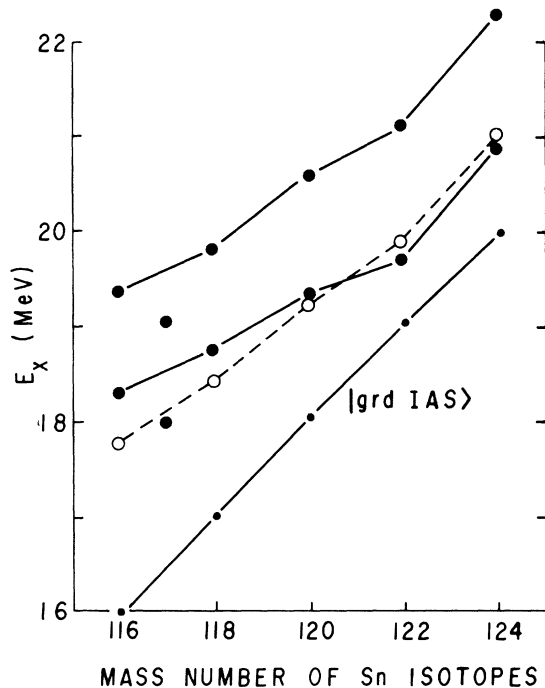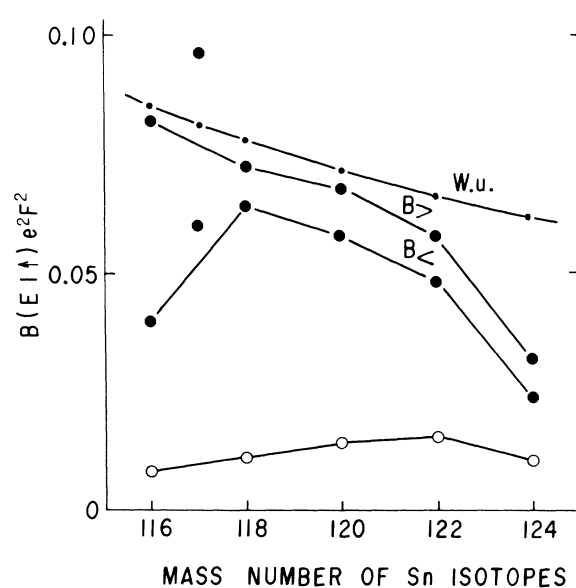

FIG. 6. Mass-number dependence of the excitation energy of the analog states. The closed circles connected with solid lines are the states found in yield-curve measurements. The open circles with dashed lines show the states found in the proton spectra. The lowest solid curve is the excitation energy of the ground analog states for even-even isotopes calculated by Eq. (6) with the semiempirical formula Eq. (7).

FIG. 7. Comparison between the reduced transition probabilities multiplied by the branching ratio Γ_p/Γ and the Weisskopf unit (W.u.) calculated by Eq. (5). The analog states with higher and lower excitation energy are denoted by $B_>$ and $B_<$. Both were found in the yield-curve measurements. The open circles show the values corresponding to the states found in the study of proton spectra.

mated from the proton spectra in Fig. 3. Since the analog state in the present results is considered to be $J = 1^-$, it is expected to emit only $L = 5$ protons to the ground state and $L = 0$ or 2 to the first excited state from the shell sequence in this region. In spite of such a large difference in angular momentum, which results in a hindrance of $L = 5$ proton emission,[19] the present branching ratio still shows a nonnegligible value. This can be explained if the present analog state has a significant $(1g_{9/2})^{-1} 1h_{11/2}$ component, which has a large transition strength for photoabsorption process.[20]

The spins and parities and the partial decay widths of the analog states offer valuable information as to the structure of the parent states. In order to find the corresponding parent states we have to obtain the positions of the ground analog states E_x(grd IAS). In the case of tin isotopes they are not known experimentally except for ^{116}Sn,[21] so that the energies were calculated by using the convenient equation[1]

$$E_x(\text{grd IAS}) = \Delta E_C - B_n + B_p , \qquad (6)$$

as explained in Fig. 4, where B_n is the neutron separation energy of the parent nucleus, B_p is the proton separation energy of the target nucleus, and ΔE_C is the Coulomb-displacement energy between the parent state and the analog state given by the semiempirical formula[22]

$$\Delta E_C = 1.444\ \bar{Z}/A^{1/3} - 1.13\ \text{MeV} , \qquad (7)$$

where $\bar{Z}$ is the average Z value of the two nuclei. The energy difference between the analog state and the ground analog state corresponds to the excitation energy of the parent state in the parent In nucleus. From this analysis it was concluded that the 19.2-MeV analog state in ^{120}Sn corresponds to a parent state at 1.1 MeV in ^{120}In.

E_x(grd IAS) for the other isotopes are listed in Table III and shown with solid lines in Fig. 6. The excitation energies of the other parent states were obtained by the same treatment and are given in the last column of Tables I and II, and are shown in Fig. 8 with spin assignments under the assumption of an $E1$ transition. In the case of ^{117}Sn there are two possibilities, $J = \frac{3}{2}^-$ or $\frac{1}{2}^-$, since its ground-

state spin is $\frac{1}{2}^+$. The closed circles connected with solid lines are the states found in the study of yield curves and the open circles with dashed lines correspond to those from the proton spectra.

The excitation energies of the parent states in odd-even ^{117}In are about 2 MeV higher than those of neighboring odd-odd indium isotopes, as shown in Fig. 8. Parent states in odd-even indium isotopes can be considered to consist of an $s_{1/2}$ quasineutron and the same 1^- configuration as that of odd-odd indium isotopes. On the other hand, ground states of the odd-odd indium isotopes have a configuration $[(\pi g_{9/2})^{-1} \otimes (\nu g_{7/2})]_{1^+}$, which is composed of an excess $g_{7/2}$ quasineutron compared with the ground states of odd-even isotopes. Therefore the excitation energies of the parent states in ^{117}In should be $E(s_{1/2}) + E(g_{7/2}) - \Delta E$ higher than those of neighboring odd-odd isotopes, where $E(j)$ are quasineutron energies[23] and ΔE is an extraordinarily strong coupling energy of 0.8 MeV[24] between proton-hole and quasineutron in the $[(\pi g_{9/2})^{-1} \otimes (\nu g_{7/2})]_{1^+}$ configuration required in order to lower to the ground state. From these the excitation energies of the parent states in ^{117}In are expected to be 2.0 MeV higher than those of neighboring odd-odd nuclei. This is in fairly good agreement with the experimental values. Sharp proton peaks were not identified in the proton energy spectrum of ^{117}Sn. This is probably due to the spreading of decay protons into many residual states which result from coupling of the $s_{1/2}$ quasi-

TABLE III. Excitation energies of the ground analog states.

A	116	117	118	120	122	124
E_x (grd IAS) (MeV)	15.9 (16.02)[a]	14.1	17.0	18.1	19.0	20.0

[a] From an ^{115}In$(p, n)^{115}$Sn experiment (see Ref. 21).
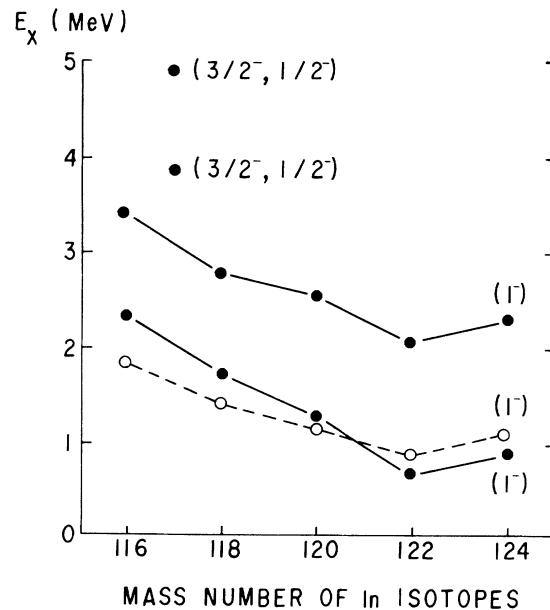

FIG. 8. The excitation energies of the parent states in In isotopes. The denoted spins and parities were assigned under the assumption of an $E1$ transition. See also the caption of Fig. 7.

neutron to the proton holes in the residual ^{116}In nucleus.

Moorhead, Cohen, and Moyer[25] studied low-lying states in ^{116}In by the reaction ^{115}In$(d, p)^{116}$In up to about 1.6 MeV and suggested the existence of a 1^- state at 1.347 MeV which has the configuration $(\pi g_{9/2})^{-1}(\nu h_{11/2})$. We could not confirm this state, although there is a small dip at 17.3 MeV just at the energy corresponding to the analog state of this level. Another dip with a similar character can be seen at about 17.6 MeV in the yield curve of ^{118}Sn.

The (γ, p) cross section of ^{120}Sn was measured previously by Kuo and Ratner.[3] The cross section reached a maximum at 20.8 ± 0.5 MeV, the width at half maximum was about 3.5 MeV, and the integrated cross section up to 30 MeV was 28 ± 3 mb MeV. Their proton-yield curve seems to show structures similar to the present ones in the cross section, but it was not analyzed from the point of view of narrow resonances. The analog states in the present result lie just in the (γ, p) giant-resonance region, and the transition strength summed up for the three states is about $\frac{1}{3}$ of the integrated cross section of Kuo and Ratner. Since the present measurement has not covered the energy region across the (γ, p) giant resonance, it is possible further analog states can be found with large transition strength in the higher-energy region, so that the total strength for all the analog resonances amounts to a considerable part of the (γ, p) cross section. However, we cannot exclude the existence of a continuous cross section which constitutes the high-energy tail of the ordinary giant resonance, because the proton yields below the ground analog-state energy are not zero and interference phenomena between the analog states and the ordinary giant resonance were found in nuclei with $N = 82$ by the present authors.[26]

ACKNOWLEDGMENT

[1] G. M. Temmer, *Fundamentals in Nuclear Theory* (International Atomic Energy Agency, Vienna, Austria, 1967), p. 163.

[2] K. Shoda, M. Sugawara, T. Saito, and H. Miyase, Phys. Letters **28B**, 30 (1968); Phys. Rev. Letters **23**, 800 (1969).

[3] Kuo Ch'i-Ti and B. S. Ratner, Zh. Eksperim. i Teor. Fiz. **39**, 1578 (1960) [transl.: Soviet Phys. – JETP **12**, 1098 (1961)].

[4] H. Yuta and H. Morinaga, Nucl. Phys. **16**, 119 (1960).

[5] J. O. Hummel, Phys. Rev. **123**, 950 (1961).

[6] R. M. Osokina, in *Proceedings of the Second All Union Conference, USSR, July, 1960* (translated by Israel Program for Scientific Translation, Jerusalem, 1966), p. 522.

[7] T. Toda, K. Irie, and I. Uetomi, Mitsubishi Denki Laboratory Reports, Mitsubishi Electric Corporation, Amagasaki, Japan, 1968 (unpublished), Vol. 9, Nos. 3 and 4.

[8] G. R. Bishop, in *Nuclear Structure and Electromagnetic Interactions*, edited by N. MacDonald (Oliver and Boyd, New York, 1965), p. 211.

[9] C. P. Browne and W. W. Buchner, Rev. Sci. Instr. **27**, 899 (1956).

[10] W. R. Dodge and W. C. Barber, Phys. Rev. **127**, 1746 (1962).

[11] W. C. Barber, Phys. Rev. **111**, 1642 (1958).

[12] R. H. Dalitz and D. R. Yennie, Phys. Rev. **105**, 1598 (1957).

[13] B. Bosco and S. Fubini, Nuovo Cimento **9**, 350 (1958).

[14] For example, in *Table of Isotopes*, edited by C. M. Lederer, J. M. Hollander, and I. Perlman (Wiley, New York, 1967), 6th ed.

[15] H. Ejiri, P. Richard, S. Ferguson, R. Hoffner, and D. Perry, Nucl. Phys. **A128**, 388 (1969).

[16] K. Shoda, A. Suzuki, M. Sugawara, T. Saito, H. Miyase, and S. Oikawa, Phys. Rev. C **3**, 1999 (1971).

[17] D. H. Wilkinson, in *Nuclear Spectroscopy*, edited by F. Ajzenberg-Selove (Academic, New York, 1960), Pt. B.

[18] B. Goulard, T. A. Hughes, and S. Fallieros, Phys. Rev. **176**, 1345 (1968).

[19] J. B. Marison and F. C. Young, *Nuclear Reaction Analysis Graphs and Tables* (North-Holland, Amsterdam, 1968).

[20] D. H. Wilkinson, Physica **22**, 1039 (1956).

[21] J. C. Thomson, K. Talbot, and G. Parry, Nucl. Phys. **89**, 209 (1966).

[22] J. D. Anderson, C. Wong, and J. W. McClure, Phys. Rev. **138**, B615 (1965).

[23] L. S. Kisslinger and R. A. Sorensen, Kgl. Danske Videnskab. Selskab, Mat.-Fys. Medd. **32**, No. 9 (1960).

[24] K. F. Alexander, in *Proceedings of the International Symposium on Nuclear Structure, Dubna, 1968* (International Atomic Energy Agency, Vienna, Austria, 1968), p. 15.

[25] J. B. Moorhead, B. L. Cohen, and R. A. Moyer, Phys. Rev. **165**, 1287 (1968).

[26] K. Shoda, T. Saito, M. Sugawara, H. Miyase, S. Oikawa, and A. Suzuki, Phys. Rev. C **4**, 1842 (1971).